

TECHNICAL UNIVERSITY OF CLUJ-NAPOCA

ACTA TECHNICA NAPOCENSIS

Series: Applied Mathematics, Mechanics, and Engineering Vol. 68, Issue Special I, May, 2025

INFLUENCE OF PHOTOPOLYMER RESIN MIXTURES ON PHYSICAL AND FRACTURE PROPERTIES

Marian-Vasile BABAN, Alexandru-Viorel COŞA, Emanoil LINUL

Abstract: This study examines the fracture behavior of Single Edge Notched Bending (SENB) specimens produced using Digital Light Processing technology. The focus is on the effect of blending two UV resins (from pure White to pure Black) on fracture properties and specimen accuracy. The research also explores crack propagation mechanisms, along with the characteristics of SENB fracture surfaces. Findings indicate that the resin mixture significantly influences the investigated properties. Among the tested specimens, W75B25 mixture shows the highest mode I fracture toughness and fracture energy, while B100 exhibits the lowest. Additionally, W25B75 and W75B25 mixtures present the smallest dimensional errors, and B100 has the lowest mass. The specimens exhibit brittle behavior, with cracks initiating from the notch tip and no observed plastic deformation.

Keywords: resin mixture, DLP, dimensional accuracy, mass, mode I fracture toughness, fracture energy.

1. INTRODUCTION

Additive manufacturing (AM) has become widespread in recent years [1-3]. 3D printing technologies like digital light processing (DLP), stereolithography (SLA), and extrusion (MEX) are used to fabricate polymer parts for various applications [4-6]. The application field of DLP printed notched specimens is quite broad, as they are relevant for various industries and products that utilize printed polymer components, such as aerospace, automotive, medical, industrial, and infrastructure. However, the energy presence of notches or geometric discontinuities in these parts can significantly impact their fracture toughness - the material's resistance to crack propagation and failure [7]. The problem is that the notch geometry and stress concentrations introduced by the notch can act as crack initiation sites, leading to premature failure of the component under loading [8]. This is a critical issue, as many structural and loadbearing applications require high toughness to ensure safe and reliable performance [9].

Most fracture mechanics studies are performed on MEX-printed specimens. Valean et al. [10] and Marsavina et al. [11] observed that factors such as the notch insertion mode, growth

direction, print orientation (PO), printer type, layer thickness (LT), specimen thickness, and filament color have a significant impact on the mode I and mode II fracture toughness values of PLA samples printed using MEX technology. In the need to recreate realistic load situations on the printed parts, Paygozar et al [12] investigates the effects of PO on the mode I fracture toughness of PLA specimens. The authors conducted three-point bending (TPB) tests on single-edge notch bending (SENB) specimens fabricated in three different POs (horizontal, lateral, and vertical) to determine the fracture toughness and fracture energy values. The results showed that the PO had a significant impact on the properties, with the horizontally printed specimens exhibiting the highest fracture toughness. Impact of printing parameters on the plane-strain fracture toughness of PLA is investigated by Milovanović et al. [13]. SENB specimens were manufactured and tested using a TPB fixture. Results indicate that infill density significantly affects fracture toughness.

Some limited studies of fracture mechanics are also found on DLP and SLA [14]. Brighenti et al. [15] experimentally studied the influence of exposure time (ET) to UV light, LT, and PO on the fracture toughness of a UV resin. The

authors concluded that careful consideration of the DLP process parameters is crucial to achieve the desired mechanical performance in load-bearing parts. Recently, mixed mode fracture tests were performed by Marghitas et al. [16] in order to simulate different loading conditions. They concluded that different fracture criteria can effectively characterize the failure under mixed mode loading conditions. The study of Khosravani et al. [17] provides insights into the fracture behavior of SLA-printed parts with different notch geometries, useful for designing AM components with improved performance.

Given the constraints in the field, this study examines the physical and fracture properties of DLP-printed SENB specimens. The primary variable is the resin mixture (White and Black), aimed at determining the optimal concentration. Additionally, a macrostructural analysis of the fracture surfaces of the tested specimens was conducted. The study of resin mixtures is motivated by economic factors and the possible improvement of fracture properties, durability, print quality and waste reduction.

2. MATERIALS AND METHODS

2.1 Materials and specimens

Standard UV-sensitive resin (ANYCUBIC Online Store 900246095, China), available in black-B and white-W, was utilized. The key properties of the resin are summarized in Table 1 according to the supplier's specifications [18].

Table 1

Main properties of used UV resins.

Property Properties of the Property	Value	Unit
UV wavelength	365-410	nm
Flexural strength	50-65	MPa
Tensile strength	36-45	MPa
Notched impact Strength	25	J/m

The geometry of the specimens was designed according to the ASTM D5045 standard [19]. The key dimensions and parameters of the SENB specimen are illustrated in Figure 1.

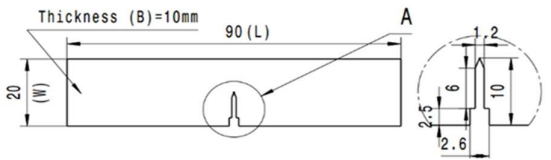


Fig. 1. SENB specimen, dimensions in mm.

2.2 Printing setup

The SENB specimens were fabricated using an Anycubic Photon Mono DLP 3D printer (Fig. 2a). This resin-based printer utilizes a monochrome LCD as the light source to cure the photopolymer resin. After printing, the parts were washed and cured using an Anycubic Wash and Cure 2.0 machine (Fig. 2b). This post-processing station is designed to streamline the cleaning and curing steps, which are essential for achieving optimal results when working with resin-based 3D printed parts, such as those produced by the Anycubic Photon series. The schematic representation of the DLP printing process is shown in Figure 2c.

The specimens were fabricated with a LT of 0.05 mm, 6 bottom solid layers, 4 s normal layer ET, and 40 s bottom layer ET. After printing, each specimen underwent a post-processing routine, which included a 10-minute wash in Isopropyl alcohol and a 20-minute curing at room temperature (25 °C) using 405 nm UV light. This post-processing step was crucial for achieving the desired part properties and ensuring the optimal final quality of the 3D printed specimens.

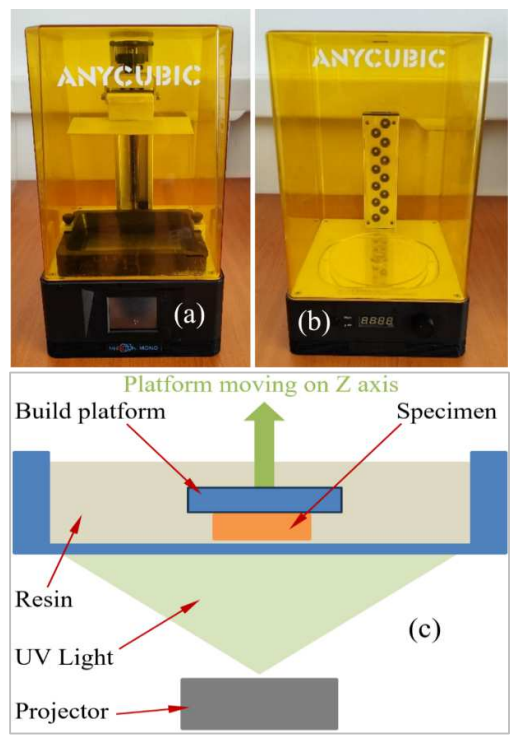


Fig. 2. Anycubic Photon Mono DLP 3D printer (a), Anycubic Wash & Cure 2.0 (b), DLP-printing process (c)

Maintaining the previously specified printing parameters, various concentrations of mixed White and Black resins were prepared as follows: 100% pure White resin (W100), 75% White + 25% Black (W75B25), 50% White + 50% Black (W50B50), 25% White + 75% Black (W25B75), and 100% Black (B100). Figure 3 shows an overview of the printed specimens. To obtain reproducibility of the results, 5 specimens were printed and tested for each configuration.

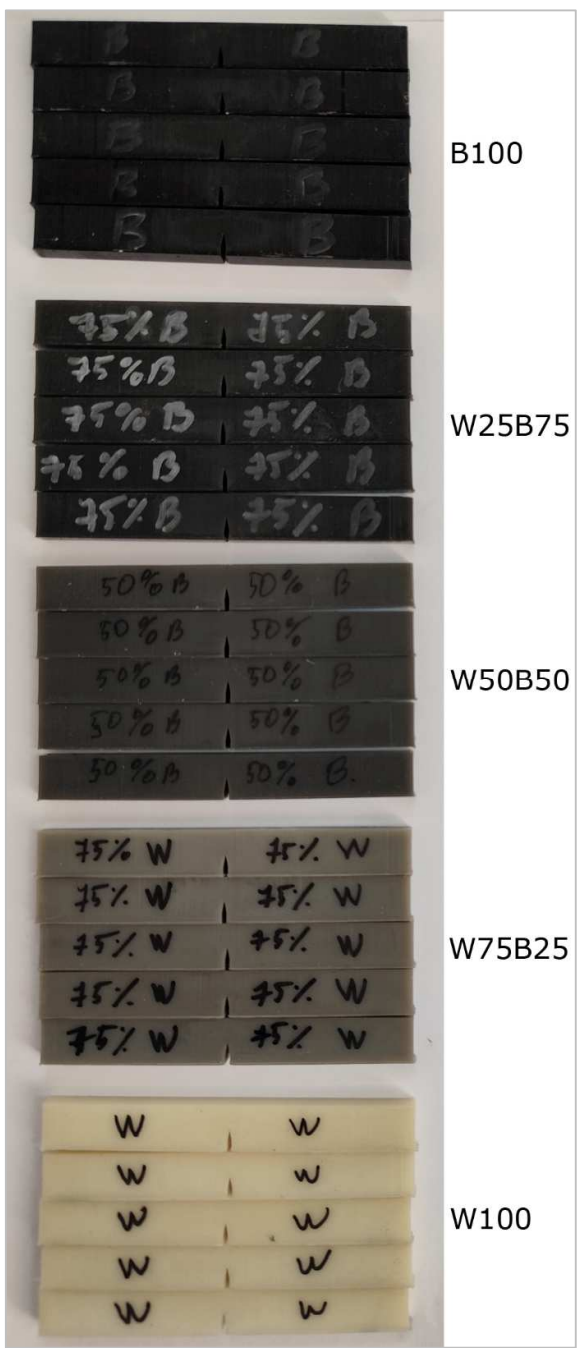


Fig. 3. DLP-printed specimens.

2.3 Methods

The experimental tests were conducted using a Metrotec universal testing machine. Figure 4 shows the experimental setup of the W100 and B100 specimens on the TPB device. The tests were performed at room temperature, with a test speed of 2 mm/min and 40 mm between the supports.

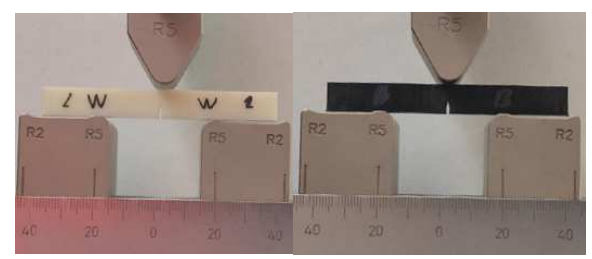


Fig. 4. TPB test setup.

The use of an ASH Digital Microscope of high-resolution enabled the capture photographs that were intended to highlight the underlying physics governing the fracture propagation process, as well as the resulting characteristics. This specialized surface microscope technology allowed for the detailed examination and documentation of the fracture mechanics and the final surface morphology that emerged from the fracturing event. The highquality imaging facilitated deeper a understanding of the complex physical phenomena during the fracture propagation, providing valuable insights through the visual data collected.

3. RESULTS AND DICUSSIONS

This section provides an analysis of the physical and mechanical characteristics of the resin mixtures under investigation. It includes evaluations of properties such as dimensional accuracy, specimen mass, mode I fracture toughness, and fracture energy. Additionally, images of the fracture surfaces of the tested specimens are presented for further examination.

3.1 Physical assessment

Figure 5 shows the variation of the relative dimensional errors with the variation of the resin mixture. The width and height errors of the printed specimens were taken into account [20].

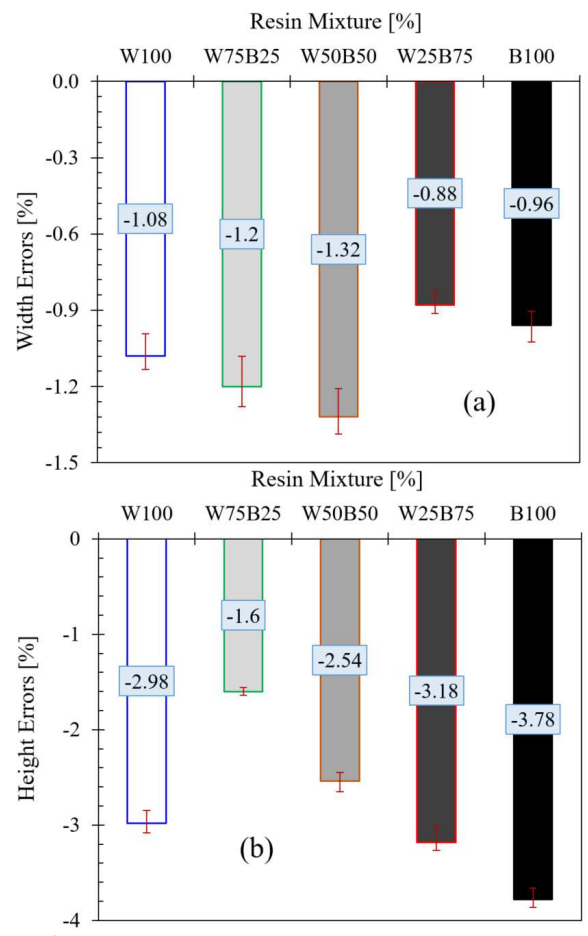


Fig. 5. Variation of dimensional errors with mixture.

The reference values considered were 5 mm for width and 10 mm for height. It can be seen that the smallest width errors are given by W25B75 mixture, and the largest by W50B50 mixture (see Fig. 5a). On the other hand, the minimum height errors are found for mixture W75B25, and the maximum for pure Black resin (see Figure 5b). As a general conclusion, it was obtained that all the measured dimensions are smaller than the nominal ones. It can also be noted that the height errors are larger than the width ones. The largest difference, approximately 4 times, found predominantly Black specimens (pure B100 resin and W25B75 mixture).

Figure 6 shows the variation of the mass of the specimens with the adopted mixture. The mass of the specimens is quite grouped, obtaining a standard deviation of only 0.04g. However, it can be seen that the heaviest specimen is obtained with W75B25 mixture, and the lightest with pure Black resin (B100).

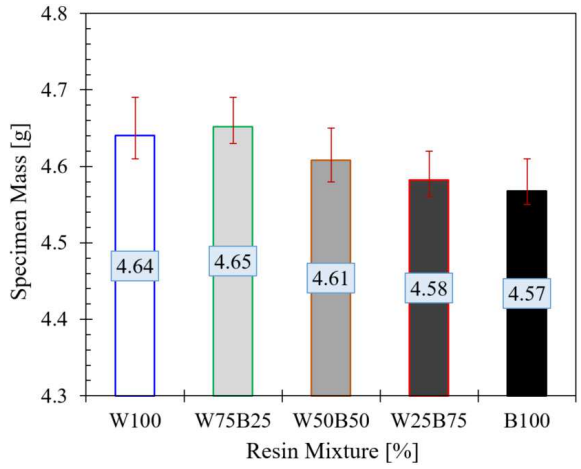


Fig. 6. Variation of specimen mass with mixture.

3.2 Mechanical assessment

Figure 7 presents the force (F) – displacement (Δ) curves for the two resin mixtures, obtained from TPB tests. All recorded F- Δ curves exhibit a characteristic brittle fracture behavior, where an initial linear-elastic response is followed by an abrupt fracture. Among the tested specimens, the W75B25 mixture shows the highest stiffness, exhibiting the steepest initial slope under TPB loading of the SENB specimens. This is followed by the W100 mixture, while B100 is identified as the least stiff.

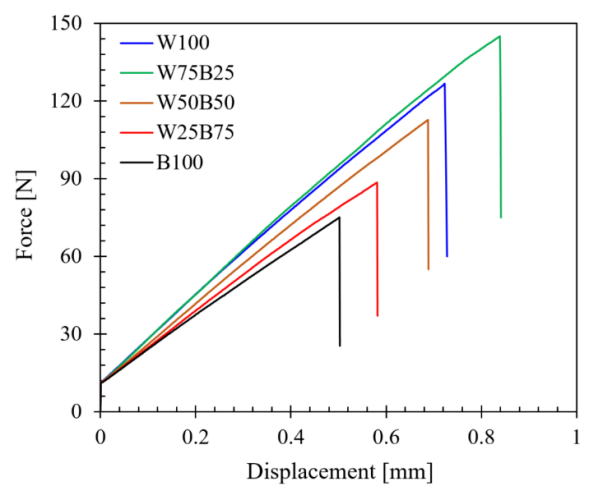


Fig. 7. Force-displacement curves.

Since the total energy absorbed by the SENB specimens corresponds to the area under the F- Δ curves, the fracture energy (G_f) trend follows the same hierarchical order as the stiffness of the different mixtures (see Fig. 8). However, for Δ

below 0.3 mm, the G_f - Δ curves for all the studied mixtures show minimal divergence, closely overlapping and indicating similar G_f behavior in the initial stage of loading.

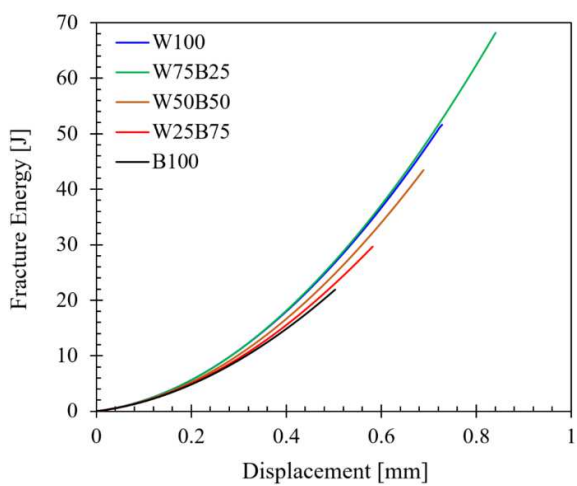


Fig. 8. Fracture energy-displacement curves.

To evaluate the mode I fracture toughness (K_{IC}) , the maximum applied force (F_Q) , identified as critical load), specimen geometrical parameters (width and height), and crack length (a) were incorporated into the Eq. (1) [19].

$$K_{IC} = \frac{F_Q}{BW^{0.5}} f\left(\frac{a}{W}\right), [MPa \cdot m^{0.5}]$$
 (1)

The geometric f(a/W) factor was computed in accordance with Eq. (2) to account for specimen geometry and loading conditions.

$$f\left(\frac{a}{W}\right) = 6\sqrt{\frac{a}{W}} \frac{1.99 - (a/W)(1 - a/W)[2.15 - 3.93(a/W) + 2.7(a/W)^2]}{(1 + 2a/W)(1 - a/W)^{1.5}} \tag{2}$$

After performing these calculations, the resulting K_{IC} values for each resin mixture were graphically represented in Figure 9. The W75B25 mixture exhibits the highest K_{IC} , reaching a maximum value of 3.48 MPa·m^{0.5}, which is 17.5% greater than that of the W100 (pure White resin). As the proportion of Black resin increases, the K_{IC} follows a polynomial decay, ultimately decreasing by more than 56% in the pure Black resin (B100). The most significant K_{IC} reduction, slightly exceeding 38%, is noted between W75B25 and W50B50

mixtures, as well as between W50B50 and W25B75 mixtures, indicating a nonlinear loss in $K_{\rm IC}$ as the Black resin content increases.

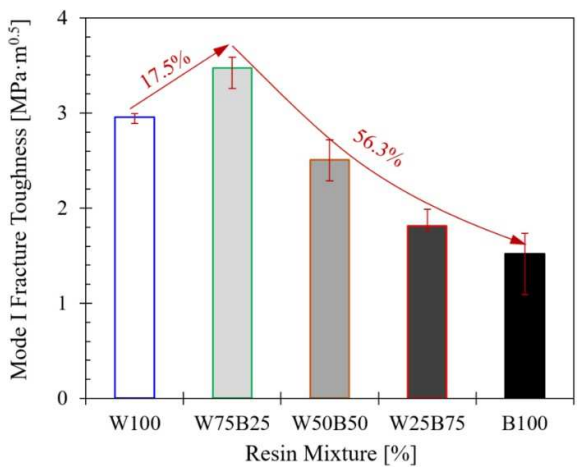


Fig. 9. Mode I fracture toughness variation.

Figure 10 shows the G_f as a function of resin mixture. The observed pattern closely correlates with the K_{IC} trend, reinforcing the relationship between stiffness and energy dissipation during fracture. The W75B25 mixture achieves the highest recorded G_f of 76.51 J, exhibiting a significantly enhanced resistance to crack propagation compared to the other mixtures. In this case, the G_f of W75B25 is 53.1% higher than that of pure White resin (W100), indicating a substantial improvement in fracture resistance due to the partial incorporation of Black resin. Conversely, the transition from the W75B25 mixture to pure Black resin results in a total G_f reduction of 76.6.

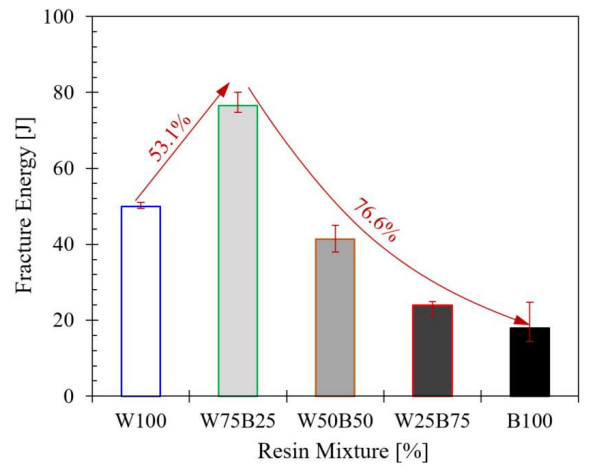


Fig. 10. Fracture energy variation.

The most pronounced G_f losses occur between W75B25 and W50B50 mixtures, where a 55% reduction is recorded, and between W50B50 and W25B75 mixtures, where the G_f decreases by 45%.

These findings suggest that while the W75B25 mixture provides an optimal balance between stiffness, K_{IC}, and G_f, increasing the content of Black resin beyond this threshold (25%) leads to significant reductions in fracture performance. A possible explanation lies in the distinct light interactions of the UV resins, where their combination optimizes curing depth and minimizes internal stresses that could cause premature cracking. Additionally, variations in crosslinking density influence the polymer network, with a balanced distribution enhancing absorption and delaying stress crack propagation, improving fracture resistance. Finally, differences in stiffness, strength and ductility affect mechanical behavior, and a wellmixed formulation allows these properties to complement each other, achieving an optimal strength-toughness balance.

Figure 11 presents macroscopic images of crack initiation, crack propagation (CP), and fracture surfaces (FS) in the tested specimens. The crack initiates (CT) from the notch tip of the **Specimens SENB** specimens. predominantly Black color (B100, W25B75 and W50B50) exhibit a more linear CP, suggesting a more direct propagation. In contrast, the pure White (W100) and W75B25 specimens display a less consistent, more curved CP, indicating a difference in the way the crack progresses through the material. The fracture surfaces (FSs) display a shiny area, with no signs of plastic deformation. Both the F- Δ curves (Figure 7) and FSs (Figure 11) indicate the brittle behavior of the specimens. The higher light absorption of black resin promotes increased polymerization rates and denser crosslinking, while the scattering effect of white resin ensures more uniform curing, and their combination likely optimizes curing depth, thereby minimizing internal stresses that could otherwise induce premature cracking.

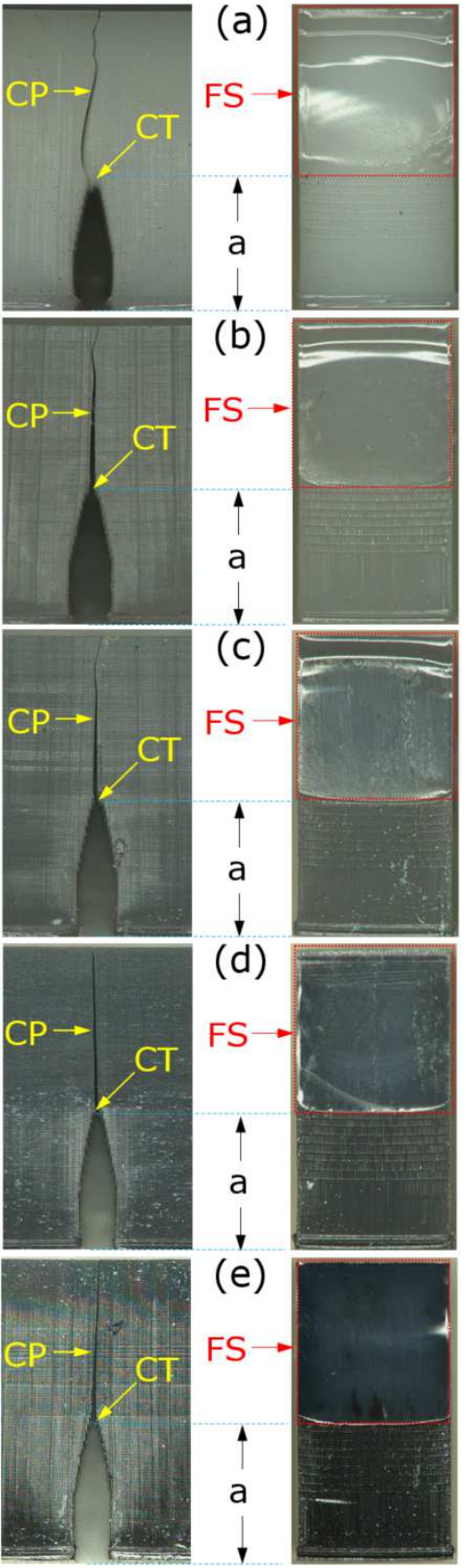


Fig. 11. Fractured W100 (a), W75B25 (b), W50B50 (c), W25B75 (d) and B100 (e) specimens.

4. CONCLUSIONS

The study explores the impact of blending two resins (White and Black) in varying proportions on their fracture properties. Based on the analysis, the following conclusions can be drawn:

- The 3D printed specimens show good dimensional accuracy, with maximum errors within acceptable standards.
- Depending on the mixture, height errors can be up to four times larger than width errors.
- The specimen mass is minimally affected by the mixture type; however, mixture W75B25 produces the heaviest specimen, while pure Black results in the lightest.
- The force-displacement curves exhibit a linear-elastic behavior with brittle failure.
- W75B25 mixture provides the optimal balance between investigated fracture properties.
- The crack path is characteristic of mode I fracture, with the specimens showing no signs of plastic deformation.
- As the Black resin content increases, fracture properties decrease, while B100 shows the weakest performance.

5. REFERENCES

- [1] Vălean, C., Marşavina, L., Linul, E., Compressive behavior of additively manufactured lightweight structures: Infill density optimization based on energy absorption diagrams, Journal of Materials Research and Technology 33, 4952-4967, 2238-7854, 2024.
- [2] Zisopol, DG., Nae, I., Portoaca, AI. Compression behavior of FFF printed parts obtained by varying layer height and infill percentage. Engineering, Technology & Applied Science Research 12(6), 9747-51, 2022.
- [3] Sergiu, C., Vitalie G., Alina B., et al., *Technological* aspects additive of manufacturing of mechanical gears: 3D printing accuracy of surfaces and dimensional chain, Acta Technica Napocensis **Applied** Mathematics,

- Mechanics and Engineering, 66, 355-364, 2023.
- [4] Vălean, C., Baban, M., Rajak, DK. et al., Effect of multiple process parameters on optimizing tensile properties for material extrusion-based additive manufacturing, Elsevier, Construction and Building Materials, 414, 135015, 2024.
- [5] Csekei, M., Šido, J., Nižňan, P., Ružarovský, R., Michal, D. *Comparison of the quality of 3d printing by robotic arm and conventional 3D printers*, Acta Technica Napocensis Applied Mathematics, Mechanics and Engineering, 67, 405-412, 2024.
- [6] Vălean, C., Orbulov, IN., Kemény, A., et al., Low-cycle compression-compression fatigue behavior of MEX-printed PLA parts, Engineering Failure Analysis, 161, 108335, 2024.
- [7]Bahrami, B., Ayatollahi, MR., Sedighi, I. *The effect of in-plane layer orientation on mixed-mode I-II fracture behavior of 3D-printed poly-carbonate specimens*, Engineering Fracture Mechanics, 231, 107018, 2020.
- [8] Ayatollahi, MR., Nabavi-Kivi, A., Bahrami, B., et al. *The influence of in-plane raster* angle on tensile and fracture strengths of 3Dprinted PLA specimens, Engineering Fracture Mechanics, 237, 107225, 2020.
- [9] Khan, AS., Ali, A., Hussain, G., Ilyas, M., An experimental study on interfacial fracture toughness of 3-D printed ABS/CF-PLA composite under mode I, II, and mixed-mode loading, Journal of Thermoplastic Composite Materials, 34; 1-24, 2019.
- [10] Vălean, C., Marşavina, L., Mărghitaș, M., et al., *The effect of crack insertion for FDM printed PLA materials on Mode I and Mode II fracture toughness*, Procedia Structural Integrity, 28, 1134-1139, 2020.
- [11] Marşavina, L., Vălean, C., Mărghitaş, M., et al., Effect of the manufacturing parameters on the tensile and fracture properties of FDM 3D-printed PLA specimens, Engineering Fracture Mechanics, 274, 108766, 2024.
- [12] Paygozar, B., Gorguluarslan, R.M., Effects of print orientation on mode-I fracture toughness of additively manufactured PLA: Simulation by XFEM, Procedia Structural Integrity, 61, 232-240, 2024.

- [13] Milovanović, A., Golubović, Z., Trajković, I., et al., *Influence of printing parameters on the eligibility of plane-strain fracture toughness results for PLA polymer*, Procedia Structural Integrity, 41, 290-297, 2022.
- [14] Baban, M.V., Coşa, A.V., Linul, E., Effect of different parameters on mode I fracture toughness of resin samples manufactured by DLP, IOP Conference Series: Materials Science and Engineering 1319, 012018, 2024.
- [15] Brighenti, R., Marsavina, L., Marghitas, et al., The effect of process parameters on mechanical characteristics of specimens obtained via DLP additive manufacturing technology, Materials Today: Proceedings, 78, 331-336, 2023.
- [16] Marghitas, M., Marsavina, L., Popa, et al., On the mixed mode fracture of DLP

- manufactured SCB specimens, Procedia Structural Integrity, 56, 26-32, 2024.
- [17] Khosravani, M.R., Frohn-Sörensen, P., Schwarzkopf, A., et al. *Brittle fracture of notched components fabricated by stereolithography*, Journal of Materials Research and Technology, 33, 8071-8078, 2024.
- [18] https://a.aliexpress.com/_ExGBL3m (accessed on march 10, 2025).
- [19] ASTM D5045, Standard test methods for plane-strain fracture toughness and strain energy release rate of plastic materials, 1999.
- [20] Vălean, C., Linul, E., Rajak, D.K., Compressive performance of 3D-printed lightweight structures: Infill pattern optimization via Multiple-Criteria Decision Analysis method, Results in Engineering, 25, 103936, 2025.

Influența amestecurilor de rășini fotopolimerice asupra proprietăților fizice și la rupere

Acest studiu analizează comportamentul la rupere al epruvetelor de încovoiere cu crestatură laterală (SENB) fabricate prin tehnologia Digital Light Processing. Accentul se pune pe efectul amestecului a două rășini UV (de la alb pur la negru pur) asupra proprietăților la rupere și acurateței dimensionale a epruvetelor. Cercetarea explorează, de asemenea, mecanismele de propagare a fisurii, precum și caracteristicile suprafețelor de rupere ale epruvetelor SENB. Rezultatele indică faptul că amestecul de rășini influențează semnificativ proprietățile investigate. Dintre probele testate, amestecul W75B25 prezintă cea mai mare tenacitate la rupere în modul I și energie la rupere, în timp ce B100 prezintă cea mai scăzută valoare. În plus, amestecurile W25B75 și W75B25 evidentiază cele mai mici erori dimensionale, iar B100 are cea mai mică masă. Epruvetele prezintă un comportament fragil, cu fisuri inițiate de la vârful crestăturii și fără deformare plastică observată.

Cuvinte cheie: amestec de rășini, DLP, precizie dimensională, masă, rezistență la rupere în modul I, energie de rupere.

- Marian BABAN, PhD Student, Politehnica University Timisoara, Department of Mechanics and Strength of Materials, marian.baban@student.upt.ro.
- **Alexandru-Viorel COŞA,** PhD Student, Assistant Professor, Politehnica University Timisoara, Department of Materials and Manufacturing Engineering, alexandru.cosa@upt.ro.
- **Emanoil LINUL,** PhD, Professor, Politehnica University Timisoara, Department of Mechanics and Strength of Materials, emanoil.linul@upt.ro.